Neurobiology of Disease

Distinct Factors Drive the Spatiotemporal Progression of Tau Pathology in Older Adults

Jenna N. Adams,[1] Theresa M. Harrison,[1] Anne Maass,[1,2] Suzanne L. Baker,[3] and William J. Jagust[1,3]
[1]Helen Wills Neuroscience Institute, University of California, Berkeley, Berkeley, California 94720, [2]German Center for Neurodegenerative Diseases (DZNE), 39120 Magdeburg, Germany, and [3]Lawrence Berkeley National Laboratory, Berkeley, California 94720

Mechanisms underlying the initial accumulation of tau pathology across the human brain are largely unknown. We examined whether baseline factors including age, amyloid-β (Aβ), and neural activity predicted longitudinal tau accumulation in temporal lobe regions that reflect distinct stages of tau pathogenesis. Seventy cognitively normal human older adults (77 ± 6 years, 59% female) received two or more ^{18}F-flortaucipir (FTP) and ^{11}C-Pittsburgh Compound B (PiB) PET scans (mean follow-up, 2.5 ± 1.1 years) to quantify tau and (Aβ). Linear mixed-effects models were used to calculate the slopes of FTP change in entorhinal cortex (EC), parahippocampal cortex (PHC), and inferior temporal gyrus (IT), and slopes of global PiB change. Thirty-seven participants underwent functional MRI to measure baseline activation. Older age predicted EC tau accumulation, and baseline EC tau levels predicted subsequent tau accumulation in EC and PHC. In IT, however, baseline EC tau interacted with Aβ to predict IT tau accumulation. Higher baseline local activation predicted tau accumulation within EC and PHC, and higher baseline hippocampal activation predicted EC tau accumulation. Our findings indicate that factors predicting tau accumulation vary as tau progresses through the temporal lobe. Older age is associated with initial tau accumulation in EC, while baseline EC tau and neural activity drive tau accumulation within medial temporal lobe. Aβ subsequently facilitates tau spread from medial to lateral temporal lobe. Our findings elucidate potential drivers of tau accumulation and spread in aging, which are critical for understanding Alzheimer's disease pathogenesis.

Key words: **aging; Alzheimer's disease; amyloid-β; fMRI; PET; tau**

Significance Statement

To further understand the mechanisms leading to tau pathogenesis and spread, we tested whether baseline factors such as age, amyloid-β pathology, and activation predicted longitudinal tau accumulation in cognitively normal older adults. We found that distinct mechanisms contribute to tau accumulation as tau progresses across the temporal lobe, with initial tau accumulation in entorhinal cortex driven by age and subsequent spread driven by neural activity and amyloid-β. We demonstrate that higher baseline activation predicts increased longitudinal tau accumulation, providing novel evidence that activation-dependent tau production may occur in the human brain. Our findings support major hypotheses generated from preclinical research, and have important translational implications, suggesting that the reduction of hyperactivation may help prevent the development of tau pathology.

Introduction

Tau and amyloid-β (Aβ) proteins, the two defining pathologies of Alzheimer's disease (AD), begin to accumulate in the brain decades before the onset of clinical impairment (Braak and Braak, 1991; Jack et al., 2010). The factors that lead to the initial accumulation and spread of these proteins in the aging brain are still not fully characterized. Using positron emission tomography (PET) and targeted radiotracers for tau and Aβ, these phenomena can now be studied with longitudinal *in vivo* data (Schöll et al., 2016, 2019).

While Aβ arises multifocally across association cortex, cortical tau accumulation first occurs in the transentorhinal region of the medial temporal lobe (MTL) and is present in nearly all older adults (Braak and Braak, 1991, 1997). In some individuals, tau

Received Aug. 5, 2021; revised Dec. 3, 2021; accepted Dec. 8, 2021.
Author contributions: J.N.A., T.M.H., and W.J.J. designed research; J.N.A. and T.M.H. performed research; J.N.A., T.M.H., A.M., and S.L.B. analyzed data; J.N.A. wrote the paper.
This research was supported by the National Institutes of Health Grants F31-AG-062090 (to J.N.A.); F32-AG-057107 (to T.M.H.); and R01-AG-034570 and R01-AG-062542 (to W.J.J.). Support was also provided by the Tau Consortium (to W.J.J.) and Helmholtz Postdoc Grant PD-306 (to A.M.). Avid Radiopharmaceuticals enabled the use of the ^{18}F-flortaucipir tracer, but did not provide direct funding and were not involved in data analysis or interpretation.
W.J.J. served as a consultant to Biogen, Genentech, and Bioclinica. S.L.B. serves as a consultant to Genentech. The authors declare no other competing financial interests.
Correspondence should be addressed to Jenna N. Adams at jnadams@berkeley.edu.
https://doi.org/10.1523/JNEUROSCI.1601-21.2021

subsequently spreads out of MTL to regions such as inferolateral temporal lobe, associated with Aβ pathology and reflecting the onset of preclinical AD (Braak and Braak, 1991; Jagust, 2018). Previous investigations of longitudinal tau-PET have largely focused on cognitively impaired individuals (Jack et al., 2018, 2020; Cho et al., 2019; Pontecorvo et al., 2019; Smith et al., 2020), in whom tau is already ubiquitous throughout temporal lobe and this distinct spatiotemporal progression can no longer be measured. While our laboratory, and others, have identified longitudinal changes in tau in the temporal lobe in cognitively normal older individuals (Hanseeuw et al., 2019; Harrison et al., 2019a; Sanchez et al., 2021), mechanisms driving pathologic tau accumulation in its earliest stages are still obscure.

An appealing model based on existing human and animal data posits that tau spreads from the entorhinal cortex to anatomically connected downstream temporal regions (De Calignon et al., 2012; Wu et al., 2016), facilitated by Aβ (Schöll et al., 2016) and driven by neural activity (Pooler et al., 2013; Wu et al., 2016). Here we investigate this model in a cognitively normal sample using functional MRI (fMRI) and longitudinal Aβ− and tau-PET. We focus on tau accumulation within three critical temporal lobe regions that reflect distinct stages of tau pathogenesis: the entorhinal cortex, the initial site of cortical tau deposition (Braak and Braak, 1991); the parahippocampal cortex, an MTL region that may develop early tau pathology because of strong connectivity with entorhinal cortex (Van Hoesen et al., 1975; Braak and Braak, 1991); and the inferior temporal gyrus, a lateral temporal region where tau accumulation is likely related to Aβ and reflects the transition to preclinical AD (Schöll et al., 2016; Jagust, 2018).

Using these regions of interest (ROIs), we test several key mechanistic hypotheses of tau accumulation. First, we assess the role of demographic risk factors such as age and apolipoprotein E (*APOE*), expecting these factors to contribute to the initial accumulation of pathology within MTL. Next, we assess the impact of baseline tau and Aβ pathology on subsequent tau accumulation rates. We expected baseline entorhinal tau pathology to be related to tau accumulation in downstream regions, supporting theories of trans-synaptic spread of tau pathology. We predicted that baseline Aβ pathology would be associated with tau accumulation rates in non-MTL regions such as inferior temporal gyrus. Finally, we examined the role of neural activity in the increased production of tau pathology. We hypothesized that higher activation at baseline, assessed with fMRI, would be associated with increased local tau accumulation.

Materials and Methods

Participants

Seventy cognitively normal older adults (OAs) aged ≥60 years from the Berkeley Aging Cohort Study who had undergone longitudinal PET were included in the present study. Inclusion criteria have been described previously (Schöll et al., 2016). Aβ+ participants were preferentially selected to receive tau-PET to obtain sufficient tau variability, leading to a higher proportion of Aβ+ participants in our longitudinal tau-PET sample than the general population. In the present study, all participants underwent PET at two or more time points (Table 1) with ^{18}F-flortaucipir (FTP) and ^{11}C-Pittsburgh Compound B (PiB) to measure tau and Aβ pathology, respectively. A subsample of 38 participants received baseline fMRI while performing a memory task. The Institutional Review Boards of the University of California, Berkeley, and the Lawrence Berkeley National Laboratory approved this study. All participants provided written informed consent.

Table 1. Demographic information and baseline characteristics of the sample

	OA full sample ($n = 70$)	OA fMRI subsample ($n = 37$)	PET vs fMRI subsamples	
			t or χ^2	p
Age (years)	77.1 (5.5)	77.2 (4.6)	−0.21	0.84
Sex (F)	41 (58.6%)	24 (64.9%)	1.28	0.26
Education (years)	16.8 (1.7)	16.5 (1.8)	1.47	0.15
MMSE	28.6 (1.3)	28.8 (1.2)	0.32	0.75
Baseline global PiB DVR	1.15 (0.23)	1.14 (0.21)	0.55	0.58
Aβ+	31 (44.3%)	17 (45.9%)	0.09	0.77
APOE ε4+	21 (30.0%)	12 (32.4%)	0.22	0.64
FTP Follow-up (years)	2.5 (1.1)	2.7 (1.1)	−2.02	0.048
2/3/4 FTP time points	44/24/2	15/20/2		

OA, cognitively normal older adults; F, female; MMSE, Mini-Mental State Examination; PiB, Pittsburgh Compound B; DVR, distribution volume ratio; APOE, apolipoprotein E; FTP, Flortaucipir.

PET

PET acquisition. FTP and PiB were synthesized at the Biomedical Isotope Facility at Lawrence Berkeley National Laboratory according to previously published protocols (Mathis et al., 2003; Schöll et al., 2016), and data were acquired on a BIOGRAPH PET/CT Truepoint six scanner (Siemens). FTP scans were acquired from 80 to 100 min postinjection (four 5 min frames). PiB was acquired dynamically for 90 min postinjection (35 frames). PET images were reconstructed with an ordered subset expectation maximization algorithm, with attenuation correction, scatter correction, and 4 mm^3 smoothing.

1.5T MRI acquisition. Structural MRIs were collected for PET coregistration and processing. A whole-brain high-resolution T1-weighted volumetric magnetization-prepared rapid acquisition gradient echo (MPRAGE) image was acquired on a 1.5T Magnetom Avanto Scanner (Siemens) at Lawrence Berkeley National Laboratory (voxels = 1 mm^3; TR = 2110 ms; TE = 3.58 ms; flip angle (FA) = 15°).

FTP processing. FTP scans were processed with a longitudinal pipeline and white matter reference region, a previously described reliable and sensitive reference region for longitudinal analyses (Harrison et al., 2019a). For ROI analyses, average MRIs were processed with FreeSurfer version 5.3.0 (http://surfer.nmr.mgh.harvard.edu/). Mean standardized uptake value ratios (SUVRs) of each ROI at each time point were quantified and partial volume corrected using a modified Geometric Transfer Matrix approach to reduce the effects of off-target FTP binding on SUVR estimates in MTL (Rousset et al., 1998; Baker et al., 2017).

To measure longitudinal change in FTP, the partial volume corrected SUVR at each time point was entered into linear mixed-effects models with random effects for participant intercept and slope. The model-estimated FTP slope for each participant was extracted for entorhinal cortex (EC), parahippocampal cortex (PHC), and inferior temporal gyrus (IT). Within the subsample of participants with fMRI, one participant had an EC FTP slope that was a negative outlier (>2.5 SDs below mean), and this data point was removed from analyses within this subsample. Baseline FTP values were also generated from the longitudinal pipeline.

To replicate whole-brain patterns of FTP accumulation identified in previous work (Harrison et al., 2019a), we conducted voxelwise analyses. For each participant, voxelwise FTP slope images (non-partial volume corrected) were created by fitting linear regressions (FTP ~ years from baseline) at each voxel. Voxelwise linear mixed-effects models were not used because of a failure of model convergence in voxels with low variability. Voxelwise slope images for each participant were warped to MNI space for group-level analyses (Harrison et al., 2019a).

PiB processing. Distribution volume ratio (DVR) images were calculated with Logan graphical analysis over 35–90 min of data, normalized by a whole-cerebellar gray reference region (Logan, 2000; Price et al., 2005). Global PiB DVR was calculated at each time point from the mean of cortical FreeSurfer ROIs. Global PiB slopes were extracted from linear mixed-effects models with random effects for participant intercept and slope. Baseline Aβ status was determined with a DVR threshold of 1.065 (Mormino et al., 2012; Villeneuve et al., 2015).

Functional MRI

3T MRI acquisition. MRI was performed at the Henry H. Wheeler Jr. Brain Imaging Center with a 3T TIM/Trio scanner (Siemens Medical Systems) and a 32-channel head coil. High-resolution whole-brain structural images were acquired with T1-weighted volumetric MPRAGE (voxels = 1 mm^3; TR = 2300 ms; TE = 2.98 ms; matrix = 256 × 240 × 160; FOV = 256 × 240 × 160 mm^3; sagittal plane = 160 slices; 5 min acquisition). fMRI was acquired while participants performed a mnemonic discrimination task using visually presented objects and scenes with novel, repeated, and lure stimuli (Berron et al., 2018; Maass et al., 2019). High-resolution whole-brain functional data were acquired using T_2*-weighted gradient-echo echoplanar images (voxels = 1.54 mm^3; multiband acceleration factor 4; TR = 2400 ms; TE = 37 ms; FA = 45°; matrix = 138 × 138; FOV = 212 × 212 mm^2; interleaved acquisition = 88 slices; posterior-anterior phase encoding, two 13 min runs).

fMRI preprocessing and analysis. Preprocessing was conducted with Statistical Parametric Mapping 12 (SPM12) using a standard native space pipeline (Maass et al., 2019; Adams et al., 2021). Outlier volumes in average intensity and motion were detected with the ArtRepair Toolbox (global intensity z score = 5; movement threshold = 0.9 mm/TR) and included as spike regressors in the first-level design matrix (Lemieux et al., 2007; Power et al., 2015). A motion threshold of 20% total outlier volumes was applied (Maass et al., 2019; Adams et al., 2021), excluding one participant and resulting in a final fMRI subsample of 37 participants.

First-level analyses were performed in native space using a general linear model in SPM12 (Maass et al., 2019; Adams et al., 2021). All stimuli types, motion regressors, and outlier volumes were included as regressors. We observed some signal dropout in lateral temporal lobe (MTL was largely unaffected) and therefore applied a conservative implicit mask of 0.8 of the global signal to remove low-signal voxels. To measure activation, we contrasted all task images against a perceptual baseline condition. This general measure of activation during mnemonic discrimination was chosen because it is more likely to be generalizable to activation patterns that occur across various task states. The mean β-value was extracted for the native space EC, PHC, IT, and hippocampus (HC) FreeSurfer ROIs.

Because of time variation between fMRI and PET acquisition, the time between fMRI and baseline FTP/PiB (FTP-fMRI = 0.85 ± 1.0 years; PiB-fMRI = 0.99 ± 1.2 years) was included as a covariate in correlations between activation and baseline FTP/PiB. We also calculated the time between fMRI and baseline FTP/PiB, divided by the time interval between the baseline and final FTP/PiB (fMRI 25%/27% into FTP/PiB follow-up interval). This measure was included in correlations between activation and FTP/PiB slope.

Experimental design and statistical analyses

Analyses of demographic variables and ROI-based FTP measures were performed using SPSS version 25. Demographic variables were compared between groups using independent-samples t tests and χ^2 tests. Group-level tau accumulation was assessed with one-sample t tests, and group comparisons of tau accumulation with independent-samples t tests. Pearson partial correlations included age as a covariate in all models, and fMRI-FTP/PiB timing adjustment in correlations with activation. Multiple regression models were performed in RStudio (R version 4.0.4) with mean centered variables. Voxelwise FTP accumulation was assessed in SPM12 using a one-sample t test (gray matter explicit mask; voxel/cluster-level thresholds of $p < 0.005$; FWE, $p < 0.05$). All other results were considered significant at $p < 0.05$.

Results

Participants

Demographic and baseline characteristics of the sample are presented in Table 1. The sample was 44% Aβ+ at baseline, resulting from selective follow-up of Aβ+ participants, and the average follow-up times were as follows: FTP = 2.5 years; PiB = 2.6 years. Importantly, there were no significant differences in demographic or baseline characteristics between the PET-only and the fMRI subsamples, though the fMRI subsample had significantly longer FTP follow-up times.

Longitudinal tau accumulation in aging

We conducted a hypothesis-driven investigation of tau accumulation within three critical temporal lobe regions: EC, PHC, and IT. Individual trajectories of FTP SUVRs over time generally increased (Fig. 1*A*). Group-level FTP accumulation, quantified as FTP slopes extracted from linear mixed models, was significant in EC ($t_{(69)} = 15.35$, $p < 0.001$), PHC ($t_{(69)} = 20.84$, $p < 0.001$), and IT ($t_{(69)} = 12.53$, $p < 0.001$), depicted in Figure 1*B*. Significant FTP accumulation occurred in subgroups of both Aβ+ (EC: $t_{(30)} = 9.34$, $p < 0.001$; PHC: $t_{(30)} = 12.04$, $p < 0.001$; IT: $t_{(30)} = 7.98$, $p < 0.001$) and Aβ− (EC: $t_{(39)} = 13.45$, $p < 0.001$; PHC: $t_{(39)} = 20.58$, $p < 0.001$; IT: $t_{(39)} = 10.92$, $p < 0.001$) participants.

While our primary aim was to investigate drivers of tau accumulation in these three a priori ROIs, we additionally investigated whole-brain voxelwise FTP accumulation to compare results to our previous work (Harrison et al., 2019a). At the group level, significant FTP accumulation predominantly occurred throughout medial and lateral temporal lobes (Fig. 1*C*), overlapping with our a priori ROIs. Additional clusters were identified in left medial parietal lobe and lateral prefrontal cortex. This spatial pattern generally replicated our previous work investigating voxelwise longitudinal FTP accumulation in 42 of 70 participants from this sample (Harrison et al., 2019a).

Baseline demographic risk factors and pathology

To characterize demographic factors that may predict longitudinal tau accumulation within temporal lobe regions, we tested relationships between baseline age, sex, and *APOE* e4 genotype with FTP slope within the full sample. Higher age at baseline was significantly associated with increased FTP slope within EC ($r = 0.33$, $p = 0.005$; Fig. 2*A*), but not PHC ($r = 0.21$, $p = 0.09$) or IT ($r = 0.17$, $p = 0.17$), supporting the role of age in initial tau accumulation in EC. There was no significant difference in FTP slope between female and male participants (EC: $t_{(68)} = 0.48$, $p = 0.63$; PHC: $t_{(68)} = -0.70$, $p = 0.49$; IT: $t_{(68)} = -0.37$, $p = 0.71$). There was also no effect of *APOE* e4 genotype on FTP slope (EC: $t_{(68)} = 0.95$, $p = 0.35$; PHC: $t_{(26.57)} = 0.93$, $p = 0.36$; IT: $t_{(24.65)} = 1.08$, $p = 0.29$).

We next assessed the effect of baseline pathology on longitudinal tau accumulation. Higher baseline EC FTP was associated with increased FTP slope in EC ($r = 0.61$, $p < 0.001$) and PHC ($r = 0.54$, $p < 0.001$), but not in IT ($r = 0.16$, $p = 0.20$; Fig. 2*B*). There was no significant difference in FTP slope by baseline Aβ status in EC ($t_{(49.00)} = 1.37$, $p = 0.18$) or PHC ($t_{(44.49)} = 1.62$, $p = 0.11$), though there was a trend suggesting higher IT FTP slope in Aβ+ participants ($t_{(68)} = 1.89$, $p = 0.06$; Aβ+, 0.021 ± 0.015; Aβ−, 0.016 ± 0.021). However, the continuous relationship between higher baseline global PiB and increased FTP slope was significant in all regions (EC: $r = 0.28$, $p = 0.02$; PHC: $r = 0.26$, $p = 0.03$; IT: $r = 0.31$, $p = 0.01$; Fig. 2*C*).

To determine the relative contributions of our baseline predictors on tau accumulation, we constructed a multiple regression model predicting FTP slope in each region (Table 2, *Baseline Predictors Model*). We included significant univariate predictors (baseline age, EC FTP, and global PiB), as well as the interaction between baseline EC FTP and global PiB to determine whether Aβ facilitates tau accumulation. Both EC and PHC FTP slope were only predicted by baseline EC FTP (p values < 0.001), with no independent or interactive effects of baseline global PiB. In contrast, the interaction between baseline EC FTP and global PiB significantly predicted IT FTP slope ($p = 0.02$), indicating that Aβ may facilitate tau spread from EC to inferolateral temporal regions.

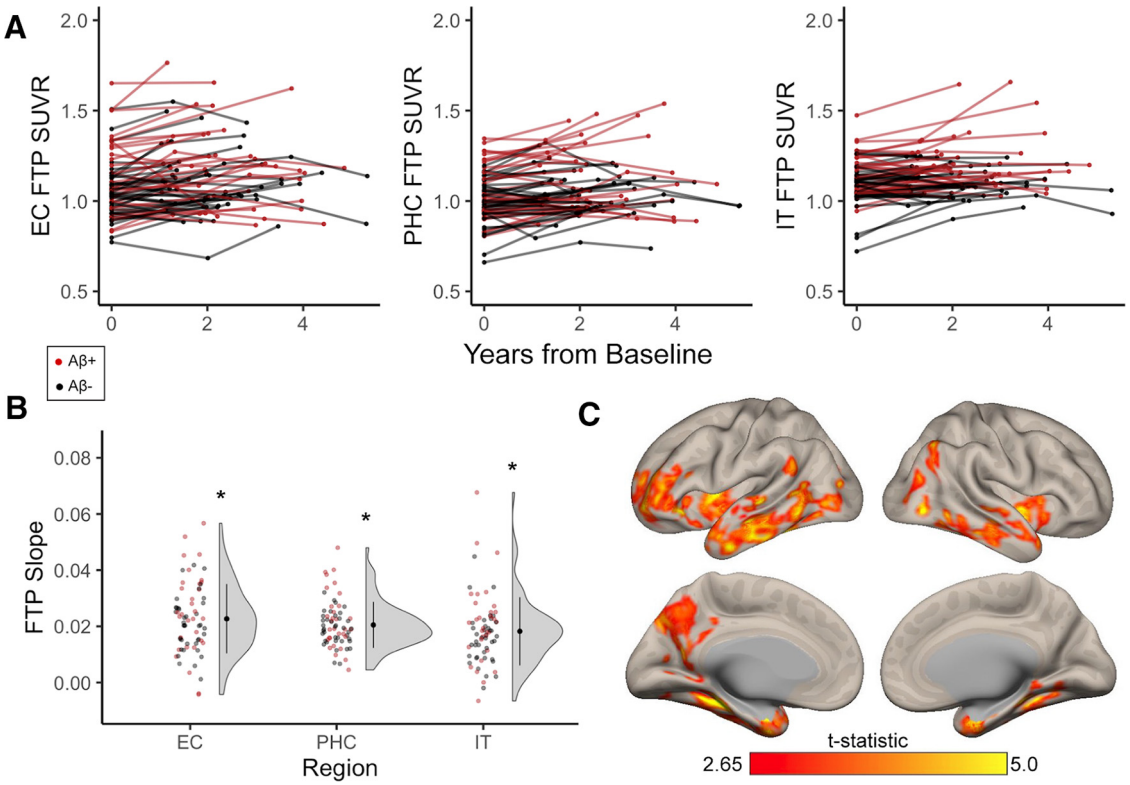

Figure 1. Longitudinal tau accumulation measured with FTP in cognitively normal older adults. Cognitively normal older adults received at least two time points of FTP, which was processed with a longitudinal pipeline. ***A***, ***B***, Red data points indicate participants who were Aβ + at baseline, while black data points indicate Aβ − participants. ***A***, Individual trajectories of FTP SUVRs over longitudinal follow-up in entorhinal cortex (EC), parahippocampal cortex (PHC), and inferior temporal gyrus (IT). ***B***, FTP slopes were computed to quantify longitudinal change in tau with linear mixed-effects models. FTP slopes were significantly greater than zero (one-sample *t* tests, $^*p < 0.001$) in EC, PHC, and IT, indicating group-level tau accumulation in these regions. ***C***, Whole-brain voxelwise FTP accumulation occurred predominantly in temporal regions (overlapping with a priori regions), but also in small clusters in medial parietal and frontal lobe, replicating previous findings in a subset of this sample. See Extended Data Figure 1-1 for whole-brain visualization of mean FTP slope in Aβ − and Aβ + groups separately.

Associations between longitudinal pathology measures

To determine how tau and Aβ pathology may temporally co-develop, we characterized associations between longitudinal accumulation of tau and Aβ pathology. We first tested whether the rate of EC FTP accumulation was associated with downstream accumulation in PHC and IT, indicating possible spread of pathology out of EC. There was a significant positive correlation between EC FTP slope and FTP slope in both PHC ($r = 0.64$, $p < 0.001$) and IT ($r = 0.47$, $p < 0.001$; Fig. 3*A*). We next tested whether the rate of global PiB accumulation was associated with FTP slope. While this association did not reach statistical significance, there was trend for a positive correlation between global PiB slope and FTP slope in each region (EC: $r = 0.22$, $p = 0.07$; PHC: $r = 0.21$, $p = 0.08$; IT: $r = 0.20$, $p = 0.095$; Fig. 3*B*).

We next tested whether EC FTP slope and global PiB slope interacted to predict downstream accumulation in PHC and IT with a multiple regression model (Table 2, *Longitudinal Predictors Model*). Both PHC and IT FTP slope were predicted by EC FTP slope (p values < 0.001), but not global PiB slope or the interaction between EC FTP slope and global PiB slope (p values > 0.05). This model indicates that the rate of change of global PiB does not contribute to FTP change in PHC or IT over and above change in entorhinal FTP.

Baseline activation as a predictor of local tau accumulation

To pursue findings from animal models that neural activity leads to the production of tau pathology (Pooler et al., 2013; Wu et al., 2016) and findings from human neuroimaging studies showing that tau is cross-sectionally associated with hyperactivation (Berron et al., 2019; Huijbers et al., 2019; Maass et al., 2019; Adams et al., 2021), we next tested whether higher baseline activation was a predictor of longitudinal tau accumulation. We examined regional fMRI activation during a memory task to investigate local activation–pathology relationships (Fig. 4). Some signal dropout in the fMRI data was observed in lateral temporal regions (Fig. 4*A*); however, we eliminated low-signal voxels before analysis (see Materials and Methods). Mean activation (β-values) was extracted for FTP ROIs to investigate local relationships with activation, and from HC for subsequent analyses (Fig. 4*B*).

We first characterized local relationships at baseline between activation and FTP. There was no significant association between levels of activation and FTP at baseline (EC: $r = 0.25$, $p = 0.15$; PHC: $r = 0.07$, $p = 0.71$; IT: $r = 0.27$, $p = 0.12$). We then tested whether baseline activation predicted local longitudinal tau accumulation. Higher baseline activation predicted local tau accumulation within EC ($r = 0.36$, $p = 0.04$) and PHC ($r = 0.38$, $p = 0.02$), but not IT ($r = 0.22$, $p = 0.20$; Fig. 4*C*), suggesting a stronger association between activation and longitudinal, rather than baseline, tau accumulation.

Because findings suggesting activation also leads to production of Aβ (Palop and Mucke, 2010), we next tested both baseline and longitudinal relationships between activation and global PiB. There was no significant baseline association between global PiB and activation in any region (EC: $r = -0.04$, $p = 0.82$; PHC: $r = 0.14$, $p = 0.44$; IT: $r = 0.16$, $p = 0.36$). However, baseline activation in IT ($r = 0.40$, $p = 0.02$) significantly predicted increased

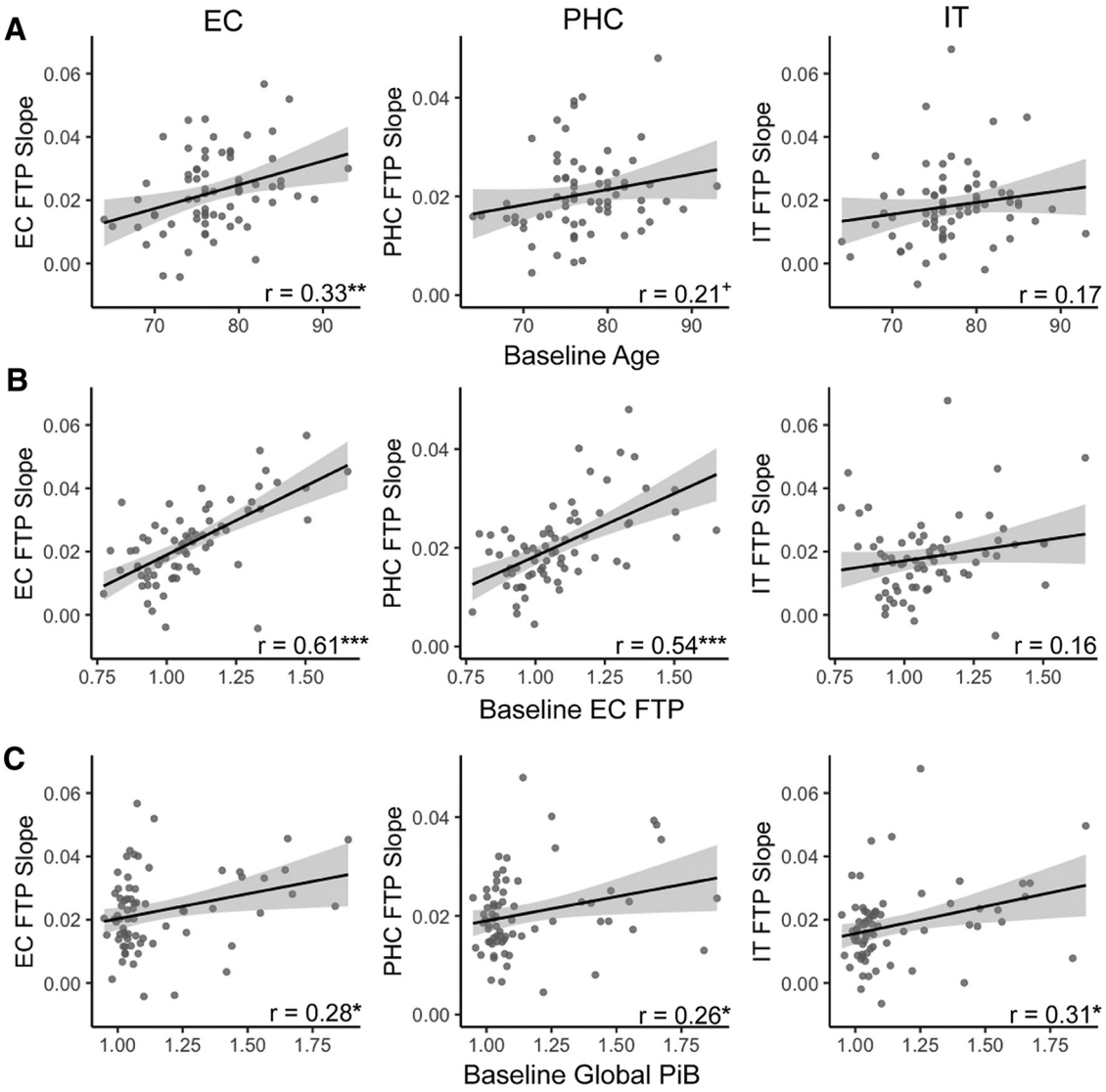

Figure 2. Baseline predictors of longitudinal tau accumulation. Pearson correlations between FTP slope, indicating the rate of longitudinal tau accumulation, and baseline risk factors. ***A***, Higher age at baseline significantly predicted increased FTP slope in entorhinal cortex (EC). ***B***, Higher baseline EC FTP was associated with increased FTP slope in EC and parahippocampal cortex (PHC), but not in inferior temporal gyrus (IT). ***C***, Higher baseline global PiB was associated with increased FTP slope in EC, PHC, and IT. ***$p < 0.001$, **$p < 0.01$, *$p < 0.05$, +$p < 0.10$.

global PiB slope, while there was a trend-level association with PHC activation ($r = 0.29$, $p = 0.09$) and no significant association with EC activation ($r = 0.14$, 0.42; Fig. 4*D*).

Because Aβ may increase activation (Busche et al., 2008), subsequently leading to tau production, we constructed a multiple regression model to test whether baseline activation interacted with baseline global PiB to predict FTP accumulation (Table 3, *Activation Model*). EC FTP slope was predicted by independent effects of baseline EC activation ($p = 0.02$) and baseline global PiB ($p = 0.003$). PHC FTP slope was predicted by baseline PHC activation ($p = 0.02$), baseline global PiB ($p = 0.001$), and by the interaction between baseline PHC activation and global PiB ($p = 0.045$). Investigating this interaction further revealed that the positive association between PHC activation and PHC FTP slope was strongest when PiB levels were low (global PiB: −1 SD, $\beta = 0.001$, $p = 0.004$; global PiB mean: $\beta = 0.000$, $p = 0.02$; global PiB: +1 SD, $\beta = 0.000$, $p = 0.82$). Finally, IT FTP slope was solely predicted by baseline global PiB ($p < 0.001$). These models demonstrate both main and interaction effects of baseline activation and Aβ on tau accumulation that vary by region.

Hippocampal activation as a biomarker of tau and Aβ accumulation

Because hippocampal activation is related to disease progression (Dickerson et al., 2005; O'Brien et al., 2010) and AD biomarkers (Berron et al., 2019; Huijbers et al., 2019; Harrison et al., 2019b; Adams et al., 2021), we additionally tested relationships between hippocampal activation and both longitudinal tau and Aβ accumulation. We first assessed baseline relationships between hippocampal activation and pathology. At baseline, higher hippocampal activation was specifically associated with greater EC FTP ($r = 0.34$, $p = 0.045$; Fig. 5*A*). There was no significant relationship between hippocampal activation and baseline PHC FTP ($r = 0.29$, $p = 0.10$), though there was a trending association with IT FTP ($r = 0.32$, $p = 0.06$). Hippocampal activation was not associated with baseline global PiB ($r = 0.14$, $p = 0.42$; Fig. 5*B*).

We next assessed relationships between baseline hippocampal activation and longitudinal accumulation of tau and Aβ. Higher hippocampal activation was associated with increased EC FTP slope ($r = 0.39$, $p = 0.02$; Fig. 5*C*), but not FTP slope in PHC ($r = 0.29$, $p = 0.10$) or IT ($r = 0.06$, $p = 0.73$). Higher baseline hippocampal activation had a trend-level relationship with increased

Table 2. Multiple regression models predicting longitudinal tau accumulation

	EC FTP slope[a]			PHC FTP slope			IT FTP slope		
	β	SE	p	β	SE	p	β	SE	p
Baseline predictors model: FTP slope ~ age + EC FTP TP1 × global PiB TP1									
Intercept	−0.000	0.001	0.99	0.000	0.001	0.86	−0.001	0.001	0.53
Age	0.000	0.000	0.06	0.000	0.000	0.63	0.000	0.000	0.08
EC FTP TP1	0.038	0.007	<0.001*	0.024	0.005	<0.001*	−0.001	0.008	0.95
Global PiB TP1	0.005	0.006	0.44	0.005	0.004	0.29	0.008	0.007	0.26
EC FTP TP1 global PiB TP1	0.002	0.02	0.94	−0.012	0.017	0.50	0.067	0.028	0.02*
Model	Adjusted R^2: 0.42			Adjusted R^2: 0.29			Adjusted R^2: 0.20		
	$F_{(65)} = 13.26$, $p < 0.001$			$F_{(65)} = 8.11$, $p < 0.001$			$F_{(65)} = 3.98$, $p = 0.006$		
Longitudinal predictors model: FTP slope ~ age + EC FTP slope × global PiB slope									
Intercept				0.000	0.001	0.80	−0.000	0.001	0.83
Age				−0.000	0.000	0.72	0.000	0.000	0.94
EC FTP Slope				0.452	0.068	<0.001*	0.460	0.122	<0.001*
Global PiB Slope				0.033	0.045	0.47	0.076	0.078	0.33
EC FTP slope × global PiB slope				−5.014	3.695	0.180	4.349	6.399	0.50
Model				Adjusted R^2: 0.43			Adjusted R^2: 0.22		
				$F_{(64)} = 13.77$, $p < 0.001$			$F_{(64)} = 5.73$, $p < 0.001$		

TP1, Time point 1 (baseline). EC, entorhinal cortex; PHC, parahippocampal cortex; IT, inferior temporal gyrus; FTP, Flortaucipir; PiB, Pittsburgh Compound B.
[a] Models predicting to EC FTP slope were not able to be performed because of the inclusion of EC FTP slope as a primary predictor.
*$p < 0.05$, significant predictor.

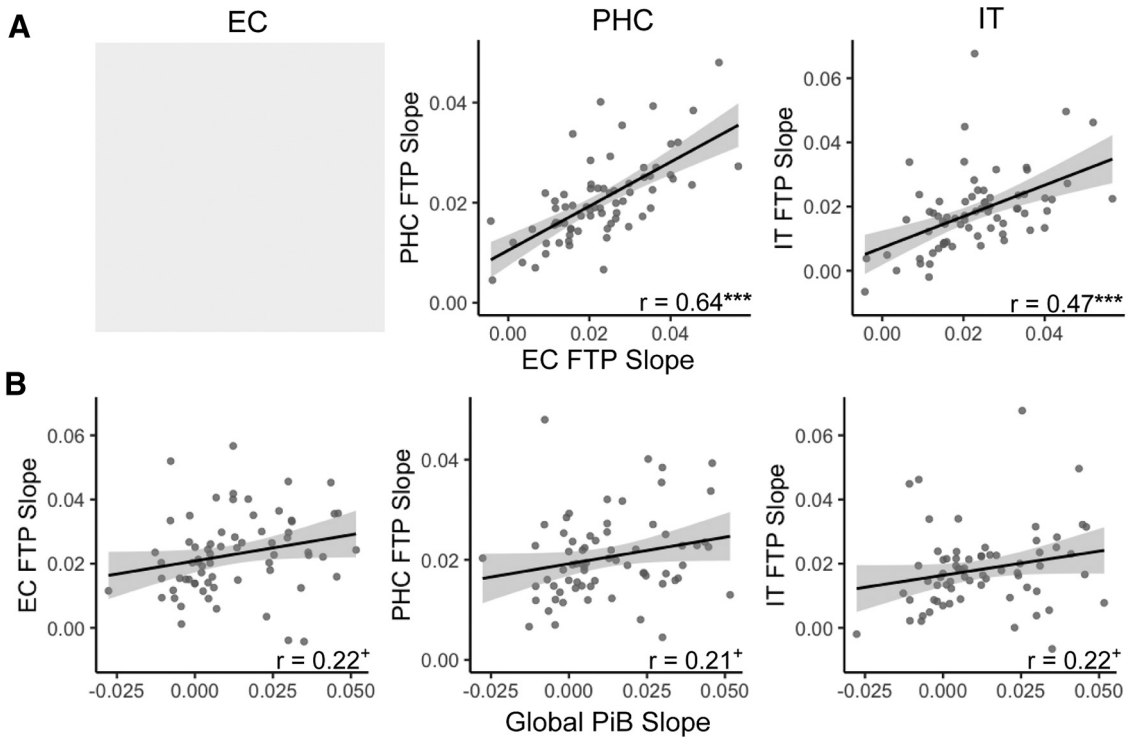

Figure 3. Longitudinal associations between tau and Aβ accumulation. ***A***, FTP slope in entorhinal cortex (EC) was highly correlated with FTP slope in parahippocampal cortex (PHC) and inferior temporal gyurs (IT). Gray shading indicates that this analysis could not be performed due to the autocorrelation between EC FTP slope. ***B***, Global PiB slope was not significantly associated with FTP slope in any region, though these associations were trending toward significance. ***$p < 0.001$, +$p < 0.10$.

global PiB slope ($r = 0.32$, $p = 0.07$; Fig. 5*D*). These results point to the specificity between hippocampal function and tau accumulation within EC.

Discussion

We demonstrate that longitudinal tau accumulation across the temporal lobe in cognitively normal older adults is driven by regionally distinct factors reflecting varying mechanisms of tau progression. Older age was associated with tau accumulation in EC, supporting initial age-related development of tau pathology. While baseline EC tau alone predicted subsequent tau accumulation within MTL, Aβ interacted with EC tau to promote tau accumulation in IT. These different patterns support that cortical tau deposition begins in the EC and spreads trans-synaptically,

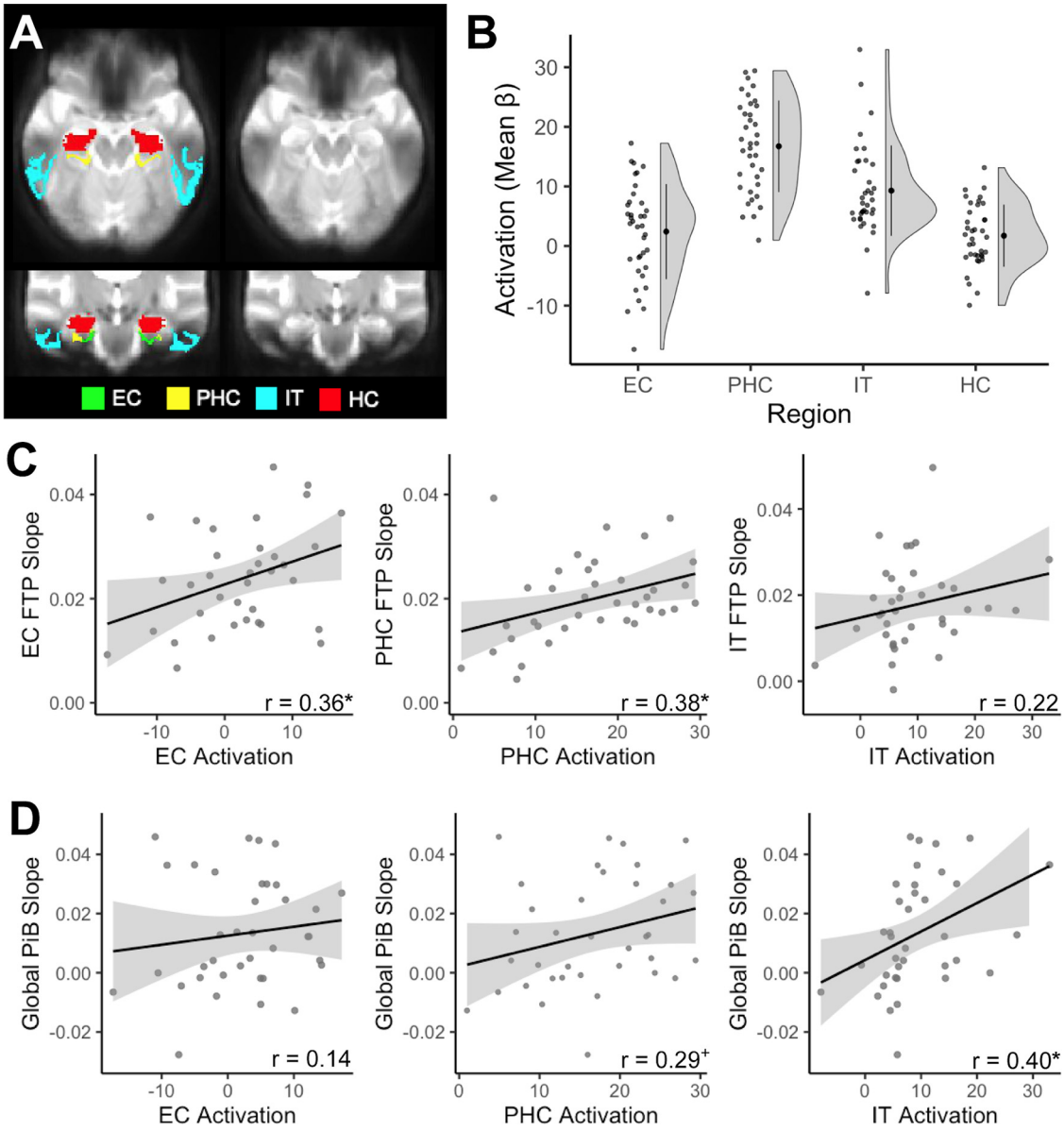

Figure 4. Local activation during memory processing and longitudinal accumulation of Alzheimer's pathology. ***A***, We investigated activity in entorhinal cortex (EC; green), parahippocampal cortex (PHC; yellow), inferior temporal gyrus (IT; cyan), and hippocampus (HC; red). Signal dropout predominantly occurred in lateral temporal regions, affecting IT; however, we removed low-signal voxels before analyses. ***B***, Activation (mean β-values) was extracted for each region, contrasting all task images against the perceptual baseline to derive a general measure of activation during memory processing. ***C***, Baseline activation was associated with increased FTP slope locally within EC and PHC, but not IT. ***D***, Baseline IT activation, but not EC or PHC activation, was associated with increased global PiB slope. $^*p < 0.05$, $+p < 0.10$.

facilitated by Aβ in its progression outside the MTL (Schöll et al., 2016). Finally, higher baseline activation significantly predicted local tau accumulation in MTL, supporting theories of activity-driven tau production (Pooler et al., 2013; Wu et al., 2016). Our results suggest that initial levels of EC tau, Aβ, and activation promote regionally dependent tau accumulation, informing on the transition from normal aging to the development of AD.

We investigated tau accumulation in three temporal lobe regions that reflect distinct stages of tau pathogenesis: EC, the initial site of cortical tau accumulation (Braak and Braak, 1991); PHC, an MTL region that develops early tau pathology (Braak and Braak, 1991); and IT, a lateral temporal region in which tau accumulation may be facilitated by Aβ and reflect the onset of preclinical AD (Schöll et al., 2016; Jagust, 2018). Importantly, we found significant group-level tau accumulation in each region, regardless of baseline Aβ status. Previous studies assessing longitudinal tau-PET have observed the highest rates of tau change in A$\beta+$ cognitively impaired samples (Jack et al., 2018, 2020; Cho et al., 2019; Pontecorvo et al., 2019; Smith et al., 2020), consistent with overall increased tau burden in these populations. Our results are consistent with recent studies demonstrating that tau accumulation is detectable within the temporal lobe in cognitively unimpaired samples (Hanseeuw et al., 2019; Harrison et al., 2019a; Sanchez et al., 2021), expanding this emerging literature.

The primary aim of this study was to assess predictors of longitudinal tau accumulation in regions that reflect distinct stages of tau progression. In EC, we found that older age strongly predicted subsequent tau accumulation. The specificity of age in predicting tau accumulation in EC, but not PHC or IT, supports cross-sectional results (Schöll et al., 2016) and theories that EC tau pathogenesis is an age-dependent process (Braak and Braak,

Table 3. Multiple regression models predicting longitudinal tau accumulation by baseline local activation

	EC FTP slope			PHC FTP slope			IT FTP slope		
	β	SE	p	β	SE	p	β	SE	p
Activation model: FTP slope ~ age + FTP-fMRI time adjustment + local activation × global PiB TP1									
Intercept	−0.000	0.001	0.98	0.000	0.001	0.76	−0.000	0.001	0.85
Age	0.001	0.000	0.11	0.000	0.000	0.07	0.000	0.000	0.27
FTP-fMRI time adjustment	0.000	0.006	0.94	−0.001	0.004	0.75	0.003	0.005	0.53
Local activation	0.000	0.000	0.02*	0.000	0.000	0.02*	0.000	0.000	0.27
Global PiB TP1	0.022	0.007	0.003*	0.019	0.005	0.001*	0.031	0.007	<0.001*
Local activation × global PiB TP1	−0.001	0.001	0.53	−0.001	0.001	0.045*	0.001	0.001	0.37
Model	Adjusted R^2: 0.28			Adjusted R^2: 0.35			Adjusted R^2: 0.43		
	$F_{(30)} = 3.73$, $p = 0.01$			$F_{(31)} = 4.86$, $p = 0.002$			$F_{(31)} = 6.48$, $p < 0.001$		

FTP-fMRI time adjustment, Time adjustment between baseline fMRI and FTP follow-up interval; TP1, time point 1 (baseline). EC, entorhinal cortex; PHC, parahippocampal cortex; IT, inferior temporal gyrus; FTP, Flortaucipir; PiB, Pittsburgh Compound B.
*$p < 0.05$, significant predictor.

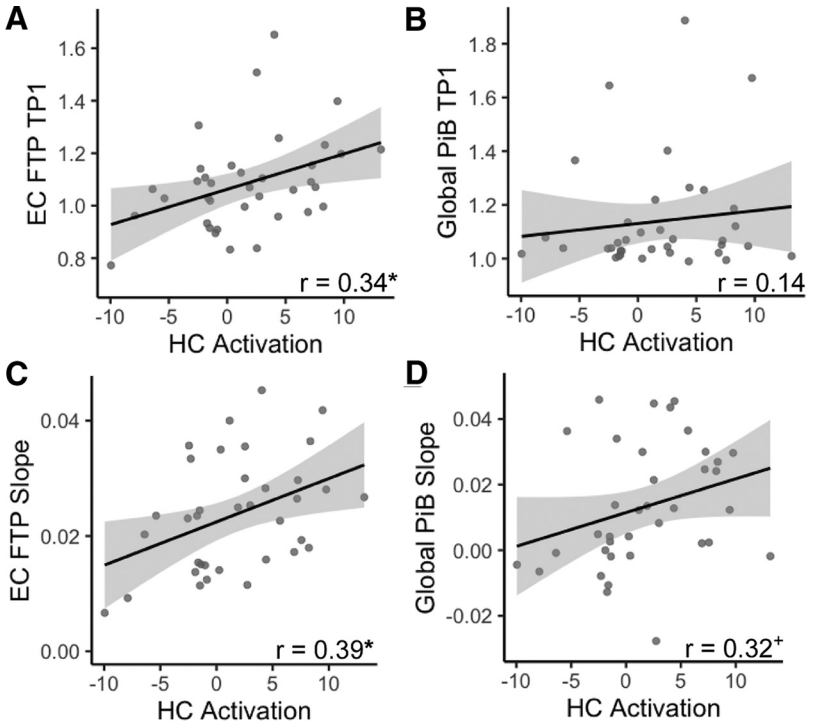

Figure 5. Hippocampal (HC) activation and longitudinal accumulation of Alzheimer's pathology. ***A***, ***B***, At baseline, increased HC activation was significantly associated with FTP in entorhinal cortex (EC) (***A***), but not global PiB (***B***). ***C***, ***D***, Higher baseline HC activation predicted increased FTP slope in EC (***C***), and a trend-level association with increased global PiB slope (***D***). *$p < 0.05$, +$p < 0.10$.

1991; Jagust, 2018). The ubiquity of EC tau deposition in aging, regardless of the co-occurrence of Aβ (Braak and Braak, 1997), suggests that tau development in this region may be a separate process from AD, known as primary age-related tauopathy (Crary et al., 2014). However, our finding that EC tau accumulation was also related to higher baseline Aβ indicates that this age-related process is subject to exacerbation, perhaps reflecting the propensity for misfolded protein aggregates to codevelop (Morales et al., 2013). Finally, we found that higher baseline EC activation predicts increased EC tau accumulation, suggesting that increased neuronal activity may play an early role in tau pathogenesis.

We next investigated predictors of tau accumulation in PHC to probe a stage of tau pathogenesis that is still contained within MTL, potentially reflecting both age- and AD-related processes. PHC tau accumulation was strongly related to baseline and change in EC tau. As PHC has strong anatomical connectivity with EC (Van Hoesen, 1982), these findings support the trans-synaptic spread of tau pathology out of EC to interconnected regions. While baseline Aβ was predictive of PHC tau accumulation in univariate models, baseline and change in EC tau predicted PHC tau accumulation over and above Aβ when included together in multivariate models. This result further supports the importance of EC tau and trans-synaptic mechanisms of tau spread within MTL. Finally, increased PHC tau accumulation was predicted by higher baseline PHC activation. Interestingly, increased PHC activation best predicted PHC tau accumulation when Aβ levels were low, suggesting that activity-driven tau production could be an early factor in MTL tau accumulation.

We assessed IT tau accumulation to investigate mechanisms driving the potential transition from normal aging to preclinical AD. Baseline Aβ, but not age or EC tau pathology, was the only univariate baseline predictor of IT tau accumulation. However, baseline Aβ interacted with baseline EC tau to predict subsequent IT tau accumulation. These findings support Aβ as a facilitator of tau progression outside the MTL, and the importance of IT tau accumulation as a potential indicator of preclinical AD. Further, we found that baseline levels of Aβ were a stronger predictor of IT tau accumulation than the rate of Aβ change, perhaps because of the relatively slower development of Aβ pathology. Finally, there was no relationship between local activation and tau accumulation in IT. This suggests that activity-related production of tau may be an earlier process that is restricted to MTL, though some fMRI signal dropout within IT may have contributed to this lack of association.

Our findings support and extend previous investigations of longitudinal tau accumulation and mechanisms of tau progression. While previous reports found differences in tau accumulation by sex (Smith et al., 2020) and *APOE* e4 positivity (Jack et al., 2020) in cognitively impaired samples, we did not observe this in our cognitively normal sample. Our findings provide longitudinal support for the trans-synaptic spread of EC tau,

consistent with animal models (De Calignon et al., 2012; Wu et al., 2016) and human neuroimaging models of tau spread based on EC functional and structural connectivity (Adams et al., 2019; Vogel et al., 2020). Additionally, our results are consistent with previous studies demonstrating associations between baseline Aβ and longitudinal tau-PET. Aβ has been shown to be a strong predictor of tau accumulation in cognitively normal participants (Jack et al., 2020), interacting with rhinal tau to predict IT tau accumulation (Sanchez et al., 2021), supporting our results.

Our results provide the first longitudinal evidence supporting activity-related tau production in the human brain. Previous neuroimaging studies have found cross-sectional associations between increased activation and tau pathology (Berron et al., 2019; Huijbers et al., 2019; Maass et al., 2019; Adams et al., 2021), speculating on the temporal directionality of this relationship. However, our data indicate a directional association where higher activation may lead to increased tau accumulation, consistent with animal models (Pooler et al., 2013; Wu et al., 2016). Hyperactivity, shown to be associated with poorer cognitive performance (Bakker et al., 2012; Berron et al., 2019), may be an intriguing target for interventional trials to prevent tau production, as reducing hyperactivation with low doses of antiepileptic drugs has been previously shown to improve memory performance in mild cognitive impairment (Bakker et al., 2012).

Hippocampal activation is a relatively reliable biomarker of disease progression, with initial hyperactivation yielding to hypoactivation as clinical symptoms of AD emerge (Dickerson et al., 2005; O'Brien et al., 2010). Additionally, hippocampal hyperactivation is related to tau pathology cross-sectionally in cognitively normal samples (Marks et al., 2017; Berron et al., 2019; Huijbers et al., 2019; Adams et al., 2021). Because of this, we assessed the relationship between hippocampal activation and longitudinal change in pathology to test whether hippocampal activation was a general predictor of overall tau accumulation. However, higher baseline hippocampal activation was exclusively associated with increased tau in EC, both longitudinally and at baseline. The specificity of this relationship to EC tau suggests that tau accumulation and neuronal activation in the EC–hippocampal circuit may be fundamentally linked. This finding replicates previous cross-sectional work (Harrison et al., 2019b; Adams et al., 2021) and further suggests that EC tau pathology may interfere with information transfer to hippocampus, disconnecting it and leading to hyperactivation (Hyman et al., 1984).

This study has several limitations. First, our sample was highly educated and enriched for amyloid positivity, which may affect the generalizability of our findings. Future studies should investigate more diverse populations with variability in health and socioeconomic outcomes to explore the relationship between lifetime health and environmental factors with longitudinal tau accumulation. Second, relationships between activation and AD pathology were conducted in a subsample of participants. However, even with reduced statistical power in this smaller sample, we were able to identify key relationships between activation and tau accumulation that are consistent with longitudinal models developed from cross-sectional human studies and preclinical research. Third, baseline PET and fMRI acquisition was not perfectly contemporaneous; however, we controlled for this time difference in all fMRI-PET analyses. Fourth, we could not assess relationships between longitudinal tau accumulation in hippocampus and activation because of FTP off-target binding in the nearby choroid plexus (Baker et al., 2017). Fifth, we could not calculate FTP slopes with linear mixed-effect models in potential control regions or in later tau-accumulating regions like medial parietal lobe. These models failed to converge because of limited variability in FTP change in these regions, suggesting a lack of FTP signal. Finally, future research should explore the heterogeneity of patterns of tau accumulation, which may not follow the more traditional "Braak-like" staging, focusing on individual-subject level patterns.

In summary, we show that temporal lobe regions reflecting different stages of tau progression have varying associations with baseline predictors. Our results support a model in which older age is most closely associated with initial cortical tau deposition in EC. Increased baseline EC tau and activation lead to further tau accumulation in MTL. Finally, Aβ facilitates tau progression out of MTL to inferolateral temporal regions. Further investigation of these predictors in larger cognitively normal samples will provide greater insight into the development of strategies to prevent or reduce tau pathology in the aging brain.

References

Adams JN, Maass A, Harrison TM, Baker SL, Jagust WJ (2019) Cortical tau deposition follows patterns of entorhinal functional connectivity in aging. Elife 8:e49132.

Adams JN, Maass A, Berron D, Harrison TM, Baker SL, Thomas WP, Stanfill M, Jagust WJ (2021) Reduced repetition suppression in aging is driven by tau-related hyperactivity in medial temporal lobe. J Neurosci 41:3917–3931.

Baker SL, Maass A, Jagust WJ (2017) Considerations and code for partial volume correcting [18F]-AV-1451 tau PET data. Data Brief 15:648–657.

Bakker A, Krauss GL, Albert MS, Speck CL, Jones LR, Stark CE, Yassa MA, Bassett SS, Shelton AL, Gallagher M (2012) Reduction of hippocampal hyperactivity improves cognition in amnestic mild cognitive impairment. Neuron 74:467–474.

Berron D, Neumann K, Maass A, Schütze H, Fliessbach K, Kiven V, Jessen F, Sauvage M, Kumaran D, Düzel E (2018) Age-related functional changes in domain-specific medial temporal lobe pathways. Neurobiol Aging 65:86–97.

Berron D, Cardenas-Blanco A, Bittner D, Metzger CD, Spottke A, Heneka MT, Fließbach K, Schneider A, Teipel SJ, Wagner M, Speck O, Jessen F, Düzel E (2019) Higher CSF tau levels are related to hippocampal hyperactivity and object mnemonic discrimination in older adults. J Neurosci 39:8788–8797.

Braak H, Braak E (1991) Neuropathological stageing of Alzheimer-related changes. Acta Neuropathol 82:239–259.

Braak H, Braak E (1997) Frequency of stages of Alzheimer-related lesions in different age categories. Neurobiol Aging 18:351–357.

Busche MA, Eichhoff G, Adelsberger H, Abramowski D, Wiederhold K, Haass C, Staufenbiel M, Konnerth A, Garaschuk O (2008) Clusters of hyperactive neurons near amyloid plaques in a mouse model of Alzheimer's disease. Science 321:1686–1689.

Cho H, Choi JY, Lee HS, Lee JH, Ryu YH, Lee MS, Jack CR, Lyoo CH (2019) Progressive tau accumulation in Alzheimer disease: 2-year follow-up study. J Nucl Med 60:1611–1621.

Crary JF, Trojanowski JQ, Schneider JA, Abisambra JF, Abner EL, Alafuzoff I, Arnold SE, Attems J, Beach TG, Bigio EH, Cairns NJ, Dickson DW, Gearing M, Grinberg LT, Hof PR, Hyman BT, Jellinger K, Jicha GA, Kovacs GG, Knopman DS, et al. (2014) Primary age-related tauopathy (PART): a common pathology associated with human aging. Acta Neuropathol 128:755–766.

De Calignon A, Polydoro M, Suárez-Calvet M, William C, Adamowicz DH, Kopeikina KJ, Pitstick R, Sahara N, Ashe KH, Carlson GA, Spires-Jones TL, Hyman BT (2012) Propagation of tau pathology in a model of early Alzheimer's disease. Neuron 73:685–697.

Dickerson BC, Salat DH, Greve DN, Chua EF, Rand-Giovannetti E, Rentz DM, Bertram L, Mullin K, Tanzi RE, Blacker D, Albert MS, Sperling RA (2005) Increased hippocampal activation in mild cognitive impairment compared to normal aging and AD. Neurology 65:404–411.

Hanseeuw BJ, Betensky RA, Jacobs HIL, Schultz AP, Sepulcre J, Becker JA, Cosio DMO, Farrell M, Quiroz YT, Mormino EC, Buckley RF, Papp KV, Amariglio RA, Dewachter I, Ivanoiu A, Huijbers W, Hedden T, Marshall GA, Chhatwal JP, Rentz DM, Sperling RA, Johnson K (2019) Association

of amyloid and tau with cognition in preclinical Alzheimer disease: a longitudinal study. JAMA Neurol 76:915–924.

Harrison TM, La Joie R, Maass A, Baker SL, Swinnerton KN, Fenton L, Mellinger TJ, Edwards L, Pham J, Miller BL, Rabinovici GD, Jagust WJ (2019a) Longitudinal tau accumulation and atrophy in aging and Alzheimer's disease. Ann Neurol 85:229–240.

Harrison TM, Maass A, Adams JN, Du R, Baker SL, Jagust WJ (2019b) Tau deposition is associated with functional isolation of the hippocampus in aging. Nat Commun 10:4900.

Huijbers XW, Schultz AP, Papp K, V., Lapoint MR, Hanseeuw X, Chhatwal XJP, Hedden T, Johnson XA, Sperling XRA (2019) Tau accumulation in clinically normal older adults is associated with hippocampal hyperactivity. J Neurosci 39:548–556.

Hyman B, Van Hoesen G, Damasio A, Barnes C (1984) Alzheimer's disease: cell-specific pathology isolates the hippocampal formation. Science 225:1168–1170.

Jack CR, Knopman DS, Jagust WJ, Shaw LM, Aisen PS, Weiner MW, Petersen RC, Trojanowski JQ (2010) Hypothetical model of dynamic biomarkers of the Alzheimer's pathological cascade. Lancet Neurol 9:119–128.

Jack CR, Wiste HJ, Schwarz CG, Lowe VJ, Senjem ML, Vemuri P, Weigand SD, Therneau TM, Knopman DS, Gunter JL, Jones DT, Graff-Radford J, Kantarci K, Roberts RO, Mielke MM, Machulda MM, Petersen RC (2018) Longitudinal tau PET in ageing and Alzheimer's disease. Brain 141:1517–1528.

Jack CR, Wiste HJ, Weigand SD, Therneau TM, Lowe VJ, Knopman DS, Botha H, Graff-Radford J, Jones DT, Ferman TJ, Boeve BF, Kantarci K, Vemuri P, Mielke MM, Whitwell J, Josephs K, Schwarz CG, Senjem ML, Gunter JL, Petersen RC (2020) Predicting future rates of tau accumulation on PET. Brain 143:3136–3150.

Jagust W (2018) Imaging the evolution and pathophysiology of Alzheimer disease. Nat Rev Neurosci 19:687–700.

Lemieux L, Salek-Haddadi A, Lund TE, Laufs H, Carmichael D (2007) Modelling large motion events in fMRI studies of patients with epilepsy. Magn Reson Imaging 25:894–901.

Logan J (2000) Graphical analysis of PET data applied to reversible and irreversible tracers. Nucl Med Biol 27:661–670.

Maass A, Berron D, Harrison TM, Adams JN, La Joie R, Baker S, Mellinger T, Bell RK, Swinnerton K, Inglis B, Rabinovici GD, Düzel E, Jagust WJ (2019) Alzheimer's pathology targets distinct memory networks in the ageing brain. Brain 142:2492–2509.

Marks SM, Lockhart SN, Baker SL, Jagust WJ (2017) Tau and β-amyloid are associated with medial temporal lobe structure, function and memory encoding in normal aging. J Neurosci 37:3192–3201.

Mathis CA, Wang Y, Holt DP, Huang GF, Debnath ML, Klunk WE (2003) Synthesis and evaluation of 11C-labeled 6-substituted 2-arylbenzothiazoles as amyloid imaging agents. J Med Chem 46:2740–2754.

Morales R, Moreno-Gonzalez I, Soto C (2013) Cross-seeding of misfolded proteins: implications for etiology and pathogenesis of protein misfolding diseases. PLoS Pathog 9:e1003537.

Mormino EC, Brandel MG, Madison CM, Rabinovici GD, Marks S, Baker SL, Jagust WJ (2012) Not quite PIB-positive, not quite PIB-negative: slight PIB elevations in elderly normal control subjects are biologically relevant. Neuroimage 59:1152–1160.

O'Brien JL, O'Keefe KM, LaViolette PS, DeLuca AN, Blacker D, Dickerson BC, Sperling RA (2010) Longitudinal fMRI in elderly reveals loss of hippocampal activation with clinical decline. Neurology 74:1969–1976.

Palop JJ, Mucke L (2010) Amyloid-beta-induced neuronal dysfunction in Alzheimer's disease: from synapses toward neural networks. Nat Neurosci 13:812–818.

Pontecorvo MJ, Devous MD, Kennedy I, Navitsky M, Lu M, Galante N, Salloway S, Doraiswamy PM, Southekal S, Arora AK, McGeehan A, Lim NC, Xiong H, Truocchio SP, Joshi AD, Shcherbinin S, Teske B, Fleisher AS, Mintun MA (2019) A multicentre longitudinal study of flortaucipir (18F) in normal ageing, mild cognitive impairment and Alzheimer's disease dementia. Brain 142:1723–1735.

Pooler AM, Phillips EC, Lau DHW, Noble W, Hanger DP (2013) Physiological release of endogenous tau is stimulated by neuronal activity. EMBO Rep 14:389–39415.

Power JD, Schlaggar BL, Petersen SE (2015) Recent progress and outstanding issues in motion correction in resting state fMRI. Neuroimage 105:536–551.

Price JC, Klunk WE, Lopresti BJ, Lu X, Hoge JA, Ziolko SK, Holt DP, Meltzer CC, DeKosky ST, Mathis CA (2005) Kinetic modeling of amyloid binding in humans using PET imaging and Pittsburgh compound-B. J Cereb Blood Flow Metab 25:1528–1547.

Rousset OG, Ma Y, Evans AC (1998) Correction for partial volume effects in PET: principle and validation. J Nucl Med 39:904–911.

Sanchez JS, Becker JA, Jacobs HIL, Hanseeuw BJ, Jiang S, Schultz AP, Properzi MJ, Katz SR, Beiser A, Satizabal CL, Donnell AO, Decarli C, Quiroz YT, Rentz DM, Sperling RA, Seshadri S (2021) The cortical origin and initial spread of medial temporal tauopathy in Alzheimer ' s disease assessed with positron emission tomography. Sci Transl Med 13: eabc0655.

Schöll M, Lockhart SN, Schonhaut DR, O'Neil JP, Janabi M, Ossenkoppele R, Baker SL, Vogel JW, Faria J, Schwimmer HD, Rabinovici GD, Jagust WJ (2016) PET imaging of tau deposition in the aging human brain. Neuron 89:971–982.

Schöll M, Maass A, Mattsson N, Ashton N, Blennow K, Zetterberg H, Jagust W (2019) Biomarkers for tau pathology. Mol Cell Neurosci 97:18–33.

Smith R, Strandberg O, Mattsson-Carlgren N, Leuzy A, Palmqvist S, Pontecorvo MJ, Devous MD, Ossenkoppele R, Hansson O (2020) The accumulation rate of tau aggregates is higher in females and younger amyloid-positive subjects. Brain 143:3805–3815.

Van Hoesen GW (1982) The parahippocampal gyrus: new observations regarding its cortical connections in the monkey. Trends Neurosci 5:345–350.

Van Hoesen GW, Pandya DN, Butters N (1975) Some connections of the entorhinal (area 28) and perirhinal (area 35) cortices of the rhesus monkey II frontal lobe afferents. Brain Res 95:25–38.

Villeneuve S, Rabinovici GD, Cohn-Sheehy BI, Madison C, Ayakta N, Ghosh PM, La Joie R, Arthur-Bentil SK, Vogel JW, Marks SM, Lehmann M, Rosen HJ, Reed B, Olichney J, Boxer AL, Miller BL, Borys E, Jin L-W, Huang EJ, Grinberg LT, et al. (2015) Existing Pittsburgh compound-B positron emission tomography thresholds are too high: statistical and pathological evaluation. Brain 138:2020–2033.

Vogel JW, Iturria-Medina Y, Strandberg OT, Smith R, Levitis E, Evans AC, Hansson O (2020) Spread of pathological tau proteins through communicating neurons in human Alzheimer's disease. Nat Commun 11:2612.

Wu JW, Hussaini SA, Bastille IM, Rodriguez GA, Mrejeru A, Rilett K, Sanders DW, Cook C, Fu H, Boonen RACM, Herman M, Nahmani E, Emrani S, Figueroa YH, Diamond MI, Clelland CL, Wray S, Duff KE (2016) Neuronal activity enhances tau propagation and tau pathology in vivo. Nat Neurosci 19:1085–1092.